CHAPTER - V

Sorption and Desorption of RG and RB on Kaolinite System

The structure of kaolinite was first suggested in general outlines by Pauling (1) and it was worked out in some detail by Gruner (2) and later revised by Brindley and his colleagues (3,4). Kaolinite belongs to the "kaolin" group of minerals and its composite sheet consists of a gibbisite layer and a silica layer. These composite sheets are lightly bound in the C-directions by H-bonding between oxygens of the tetrahedral layer of one composite sheet and the hydroxyls of the octahedral layer of the next one. Very little expansion is, thus, possible in C-direction. The basal spacing value of kaolinite is 7.37 A^{o} (5). Grim, Allaway and Cuthbert (6) observed that kaolinites enter into exchange reactions with organic ions upto their exchange capacity and showed that large organic ions added in excess of the exchange capacity tend to be adsorbed by van der Waals forces. Mortenson (7) showed that unsatisfied valence bonds of the exposed lattice aluminium are involved in the bond formation in exchange reactions.

The sorption and desorption behaviour of methylene blue, malachite green and crystal violet on and from kaolinite were studied by De, Das Kanungo and Chakravarti (8). The present study

of the sorption and desorption characteristics of RG and RB on and from kaolinite aims at gaining some more knowledge in this fascinating area.

The sorption and desorption characteristics of RG and RB on and from Na-kaolinite are discussed below. The characteristics of sorption are presented in Section A and those of desorption in Section B.

In Section A, short discussion on infrared study of both RG and RB exchanged Na-kaolinite has been included.

SECTION - A

Sorption Studies

Sorption of RG^+ on Na-kaolinite:

The adsorption isotherm of RG^+ on Na-kaolinite together with the reciprocal linear plots are given in Fig. 25(a) and 25(b) respectively. It is a typical Langmuir H-type of isotherm indicative of strong adsorbate-adsorbent interaction and adsorbed species lying flat on the surface. The dye molecules are adsorbed so strongly on the mineral surface at low concentration that the equilibrium concentration becomes negligible upto about 4 meq/100g of dye sorption. Both the value of V_m (7.1 meq/100g), calculated from the linear Langmuir plot, and the maximum sorption of the dye from the isotherm (6.9 meq/100g) are greater than the c.e.c. of the mineral (5.4 meq/100g). As observed in montmorillonite here also RG is adsorbed in excess of c.e.c. The higher uptake of RG as exaplained earlier (page 61) as a consequence of the greater association tendency of the dye in solution and the resulting sorption of aggregation and/or unionised dye molecules onto the mineral.

The adsorption is mostly due to ionic and van der Waals forces upto the c.e.c. beyond which it is solely due to van der Waals forces. The value of the Langmuir bonding constant calculated from the linear plot, is $1.75 \times 10^5 M^{-1}$.

Sorption of RB^+ on Na-kaolinite:

The sorption isotherm of RB^+ on kaolinite (Fig. 32a) is also of the Langmuir type indicating flat orientation of the adsorbed dye onto the mineral. Accordingly the plot of C/X vs C is linear [Fig. 32(b)]. From the slope of the line, the value of V_m is found to be 6.25 meq/100g which is almost equal to the value of the maximum adsorption of the dye 6.4 meq/100g obtained from the isotherm. These values though slightly lower than those of RG^+, are still higher than the c.e.c. value of Na-kaolinite. This is probably due to sorption of aggregated ions from the solution of dimerisation or stacking of dye ions over the one already present in the adsorbed state.

As mentioned before the amount of RB^+ adsorbed by Na-kaolinite is less than the amount of RG^+ adsorbed. This is perhaps due to lower aggregation tendency of RB^+ compared to RG^+ in aqueous medium (page 61) and consequently there is less amount of aggregated RB molecules adsorbed.

The computed Langmuir, constant for RB^+ on to Na-kaolinite is equal to $2.66 \times 10^5 M^{-1}$, which is higher than that of RG-Na-kaolinite system signifying that the former dye is more firmly anchored to the mineral. A similar behaviour of these dyes has been observed earlier in Na-montmorillonite.

Infrared Spectral Studies on RG^+ and RB^+ exchanged Na-kaolinite:

The infrared spectra of RG, RB, Na-kaolinite, 100% RG exchanged, 100% RB-exchanged are shown in Fig. 21, 22, 39, 40, 41 respectively. From such observations it shows that the significant ring vibration at 1580 cm^{-1} has been shifted to 1603 cm^{-1} indicating aggregation tendency of the dye in the interlayer space. Similar behaviour has been found in Na-montmorillonite (page 64).

But for RB (Fig. 22) this band which appears at 1602 cm^{-1} can not be distinguishable in 100% RB-exchange-kaolinite suggesting very little sorption of dye on the clay surface.

SECTION - B

Desorption Studies

Desorption of Rhodamine RG^+ from Na-Kaolinite -RG :

The procedure for desorption studies has already been described (page 52). Figs. 26-30 show the isotherms of desorption by various inorganic and organic ions whose selectivity coefficients and distribution coefficients are given in table 8. The exchange curve are very similar in nature to those obtained in the case of Na-montmorillonite-RG complex. The extent of release of RG^+ from the clay-matrix is directly related to the size of the desorbing ions. According to there exchange efficiency the desorbing ions may be arranged as follows: $Li^+ < Na^+ < K^+ \geq NH_4^+ < Rb^+ < Cs^+$ for monovalent, $Mg^{2+} < Ca^{2+} < Sr^{2+} < Ba^{2+}$ for bivalent ion. Interestingly the percentage of desorption of RG^+ from its Na-kaolinite complex by the monovalent and divalent inorganic ions is much higher compared to montmorillonite while it has got lower value by the larger organic ions, although the extent of desorption increases with the size of the ions in both the cases. This can be, however, understood on the basis of the structural characteristics of this mineral. In kaolinite the exchange capacity is very low and its surface area is ($\simeq 7.0\ m^2/g$) (9). The area per exchange site in kaolinite is smallest as compared to other minerals structures here.

Judging from the structural behaviour of this mineral, the exchange sites are located only on the exterior surfaces of the crystal due to its non-expansible character and the distance between two exchange sites is the smallest in this mineral. So the strength of binding of this dye with kaolinite is expected to be weak as compared to that with other minerals and owing to the close proximity of the exchange sites it may so happen that the small-sized inorganic ions can match the exchange positions more appropriately to displace the adsorbed dye. Probably small sized ions have also got less "Cover-up" effect. Conversely, the larger organic ions blanket some of the closely spaced exchange sites though higher dispersion force owing to their bigger size, tends to enhance the extent of exchange. Due to this resultant effect, the extent of desorption in kaolinite is lower than in other mineral systems studied here.

As in the desorption of RG^+ from its montmorillonite complexes, have also both $1/a^o$ and the hydrated ionic radius of the alkaline earth metal ions plotted against log (selectivity coefficient) behave linearly (Fig. 31). But for monovalent inorganic ions the plot of hydrated ionic radii vs log (selectivity coefficient) is non-linear whereas it behaves linearly (Fig. 31) when $1/a^o$ values are plotted against log (selectivity coefficient). A similar behaviour was noted earlier in the other minerals studied.

Desorption of RB^+ from Na-Kaolinite-RB :

The desorption of RB^+ from its kaolinite complex by inorganic and organic ion (Figs. 33-37) are similar to those for RG-kaolinite. The only difference is that the percentage of RG^+ desorbed as well as the calculated distribution and selectivity coefficients are higher than those of RB^+ indicating a stronger binding of latter to this clay.

According to the values of the distribution and selectivity coefficients, the inorganic ions (Table 9) may be placed in the order : $Li^+ < Na^+ < K^+ \leqslant NH_4^+ < Rb^+ < Cs^+$ for the monovalent ions, $Mg^{2+} < Ca^{2+} < Sr^{2+} < Ba^{2+}$ for the bivalent ions. The extent of RB^+ desorption is directly proportional to the size of the inorganic ions and agrees with other cases of dye desorption. The selectivity coefficients, as will be seen from the data given in Table 9 are much lower than 1.0, which indicates a much smaller affinity of the desorbing ions than RB^+ for the kaolinite surfaces. As noted earlier in the desorption of RG^+ from the Na-kaolinite-RG, here also the extent of exchange of RB^+ by monovalent and bivalent inorganic ions is much higher than in montmorillonite complex and may be explained on the basis of the difference in interchange separation of the minerals vis-a-vis the smaller size of these ions.

The percentates of release of the adsorbed dye from clay-RB complex by the large organic ions are lower in Na-Kaolinite-RB complex than in the complexes of montmorillonite. This may be interpreted in a similar manner on the basis of the proximity of the exchange sites and contribution of van der Waals forces vis-a-vis size of the ions and cover up effect as done for RG^+ desorption from its Na-Kaolinite Complex (page 95).

The plot of log selectivity coefficient against hydrated ionic radii yields straight lines for bivalent inorganic ions whereas for the monovalent inorganic ions it is non-linear (Fig. 38). However $1/a^o$ vs log selectivity coefficient plot for both monovalent and bivalent inorganic ions is linear (Fig. 38). This type of behaviour had also been found in other exchanges and its usefulness had already been discussed in page 73.

The extent of desorption of RG^+ from its kaolinite complex is higher than that of RB^+ from Na-Kaolinite-RB complex, indicating thereby a weaker binding of RG^+ to this exchanger. The higher value of Langmuir bonding constant for RB^+ is also compatible with this observation.

Such an order in the values of the bonding strengths of the two dyes in question has also been noticed in previous mineral system studied here. The explanation for this is similar which has already been discussed in the earlier case (page 75).

TABLE - 8

Desorption characteristics of RG from Na-kaolinite-RG with respect to different ions.

Electrolyte used	Concentration of electrolyte	Distribution Coefficient	Selectivity Coefficient
1:1 Electrolyte			
LiCl	0.1 (M)	1.31×10^{-2}	1.48×10^{-8}
	0.2 (M)	1.03×10^{-2}	1.74×10^{-8}
	0.3 (M)	8.08×10^{-3}	1.71×10^{-8}
	0.5 (M)	5.79×10^{-3}	1.48×10^{-8}
	0.75 (M)	4.21×10^{-3}	1.18×10^{-8}
NaCl	0.1 (M)	1.63×10^{-2}	2.30×10^{-8}
	0.2 (M)	1.13×10^{-2}	2.24×10^{-8}
	0.3 (M)	8.96×10^{-3}	2.12×10^{-8}
	0.5 (M)	6.43×10^{-3}	1.83×10^{-8}
	0.75 (M)	4.77×10^{-3}	1.53×10^{-8}
KCl	0.1 (M)	0.022	4.27×10^{-8}
	0.2 (M)	0.015	4.14×10^{-8}
	0.3 (M)	0.012	4.07×10^{-8}
	0.5 (M)	0.009	3.75×10^{-8}
	0.75 (M)	0.006	3.01×10^{-8}

TABLE -8 (Contd..)

Electrolyte used	Concentration of electrolyte	Distribution Coefficient	Selectivity Coefficient
	0.1 (M)	0.0179	2.77×10^{-8}
NH_4Cl	0.2 (M)	0.013	3.30×10^{-8}
	0.3 (M)	0.010	3.06×10^{-8}
	0.5 (M)	0.008	3.22×10^{-8}
	0.75 (M)	0.006	2.94×10^{-8}
	0.1 (M)	0.029	7.43×10^{-8}
RbCl	0.2 (M)	0.021	8.28×10^{-8}
	0.3 (M)	0.016	7.54×10^{-8}
	0.5 (M)	0.011	6.42×10^{-8}
	0.75 (M)	0.008	4.88×10^{-8}
	0.1 (M)	0.036	1.22×10^{-7}
CsCl	0.2 (M)	0.023	1.05×10^{-7}
	0.3 (M)	0.018	9.52×10^{-8}
	0.5 (M)	0.012	9.86×10^{-8}
	0.75 (M)	0.009	6.41×10^{-8}

TABLE - 8 (Contd..)

Electrolyte used	Concentration of electrolyte	Distribution Coefficient	Selectivity Coefficient
2:1 Electrolyte			
	0.05 (M)	0.180	2.47×10^{-7}
$MgCl_2$	0.10 (M)	0.155	3.30×10^{-7}
	0.20 (M)	0.123	3.30×10^{-7}
	0.30 (M)	0.103	2.95×10^{-7}
	0.40 (M)	0.090	2.66×10^{-7}
	0.05 (M)	0.210	4.06×10^{-7}
$CaCl_2$	0.10 (M)	0.162	3.76×10^{-7}
	0.20 (M)	0.123	3.30×10^{-7}
	0.30 (M)	0.104	3.07×10^{-7}
	0.40 (M)	0.092	2.83×10^{-7}
	0.05 (M)	0.220	4.47×10^{-7}
$SrCl_2$	0.10 (M)	0.167	4.11×10^{-7}
	0.20 (M)	0.130	4.00×10^{-7}
	0.30 (M)	0.107	3.34×10^{-7}
	0.40 (M)	0.097	3.36×10^{-7}

TABLE - 8 (Contd..)

Electrolyte used	Concentration of electrolyte	Distribution Coefficient	Selectivity Coefficient
	0.05 (M)	0.224	4.99×10^{-7}
$BaCl_2$	0.10 (M)	0.171	4.48×10^{-7}
	0.20 (M)	0.129	3.86×10^{-7}
	0.30 (M)	0.109	3.50×10^{-7}
	0.40 (M)	0.009	3.33×10^{-7}
Quaternary Ammonium Salts			
	0.05 (M)	0.028	3.47×10^{-8}
TMBABr	0.10 (M)	0.026	5.98×10^{-8}
	0.20 (M)	0.019	6.76×10^{-8}
	0.30 (M)	0.015	6.88×10^{-8}
	0.40 (M)	0.013	6.30×10^{-8}
	0.05 (M)	0.034	5.22×10^{-8}
TEABr	0.10 (M)	0.031	8.88×10^{-8}
	0.20 (M)	0.023	1.03×10^{-7}
	0.30 (M)	0.018	1.01×10^{-7}
	0.40 (M)	0.015	9.48×10^{-8}

TABLE - 8 (Contd..)

Electrolyte used	Concentration of electrolyte	Distribution Coefficient	Selectivity Coefficient
	0.05 (M)	0.047	9.83×10^{-8}
TPABr	0.10 (M)	0.039	1.41×10^{-7}
	0.20 (M)	0.028	1.51×10^{-7}
	0.30 (M)	0.022	1.47×10^{-7}
	0.40 (M)	0.018	1.34×10^{-7}
	0.05 (M)	0.094	4.12×10^{-7}
TBABr	0.10 (M)	0.063	3.79×10^{-7}
	0.20 (M)	0.039	3.13×10^{-7}
	0.30 (M)	0.029	2.62×10^{-7}
	0.40 (M)	0.023	2.20×10^{-7}
	2×10^{-4} (M)	9.754	1.65×10^{-5}
DDTMABr	4×10^{-4} (M)	6.852	1.65×10^{-5}
	6×10^{-4} (M)	5.542	1.63×10^{-5}
	8×10^{-4} (M)	4.743	1.61×10^{-5}
	1×10^{-3} (M)	3.956	1.41×10^{-5}

TABLE - 8 (Contd..)

Electrolyte used	Concentration of electrolyte	Distribution Coefficient	Selectivity Coefficient
	2×10^{-4} (M)	23.990	1.05×10^{-4}
CTMABr	4×10^{-4} (M)	14.496	7.88×10^{-5}
	6×10^{-4} (M)	11.420	7.50×10^{-5}
	8×10^{-4} (M)	8.828	6.01×10^{-5}
	1×10^{-3} (M)	7.174	4.96×10^{-5}
	1×10^{-4} (M)	11.336	2.24×10^{-5}
DDPBr	2×10^{-4} (M)	7.906	2.22×10^{-5}
	3×10^{-4} (M)	6.061	1.97×10^{-5}
	4×10^{-4} (M)	4.941	1.76×10^{-5}
	5×10^{-4} (M)	4.162	1.57×10^{-5}
	1×10^{-4} (M)	31.635	1.89×10^{-4}
CPBr	2×10^{-4} (M)	18.581	1.34×10^{-4}
	3×10^{-4} (M)	13.265	1.03×10^{-4}
	4×10^{-4} (M)	10.343	8.47×10^{-5}
	5×10^{-4} (M)	8.440	7.07×10^{-5}

TABLE - 9

Desorption characteristics of RB from Na-kaolinite-RB with respect to different ions.

Electrolytes used	Concentration of electrolyte	Distribution Coefficient	Selectivity Coefficient
1:1 Electrolyte			
LiCl	0.1 (M)	6.84×10^{-3}	3.80×10^{-9}
	0.2 (M)	4.73×10^{-3}	3.70×10^{-9}
	0.3 (M)	3.68×10^{-3}	3.37×10^{-9}
	0.5 (M)	2.73×10^{-3}	3.11×10^{-9}
	0.75 (M)	2.03×10^{-3}	2.59×10^{-9}
NaCl	0.1 (M)	1.05×10^{-2}	9.17×10^{-9}
	0.2 (M)	7.10×10^{-3}	8.41×10^{-9}
	0.3 (M)	5.61×10^{-3}	7.92×10^{-9}
	0.5 (M)	3.89×10^{-3}	6.38×10^{-9}
	0.75 (M)	2.94×10^{-3}	5.51×10^{-9}
KCl	0.1 (M)	1.73×10^{-2}	2.53×10^{-8}
	0.2 (M)	1.07×10^{-2}	1.96×10^{-8}
	0.3 (M)	8.06×10^{-3}	1.66×10^{-8}
	0.5 (M)	5.26×10^{-3}	1.18×10^{-8}
	0.75 (M)	3.64×10^{-3}	7.96×10^{-9}

TABLE - 9 (Contd..)

Electrolyte used	Concentration of Electrolyte	Distribution Coefficient	Selectivity Coefficient
	0.1 (M)	1.31×10^{-2}	1.44×10^{-8}
NH_4Cl	0.2 (M)	9.73×10^{-3}	1.59×10^{-8}
	0.3 (M)	8.06×10^{-3}	1.66×10^{-8}
	0.5 (M)	5.99×10^{-3}	1.54×10^{-8}
	0.75 (M)	4.27×10^{-3}	1.11×10^{-8}
	0.1 (M)	2.63×10^{-2}	5.91×10^{-8}
RbCl	0.2 (M)	1.76×10^{-2}	5.40×10^{-8}
	0.3 (M)	1.36×10^{-2}	4.94×10^{-8}
	0.5 (M)	9.78×10^{-3}	4.28×10^{-8}
	0.75 (M)	7.22×10^{-3}	3.54×10^{-8}
	0.1 (M)	3.15×10^{-2}	8.61×10^{-8}
CsCl	0.2 (M)	2.05×10^{-2}	7.41×10^{-8}
	0.3 (M)	1.59×10^{-2}	6.82×10^{-8}
	0.5 (M)	1.14×10^{-2}	5.99×10^{-8}
	0.75 (M)	8.55×10^{-3}	5.07×10^{-8}

TABLE - 9 (Contd..)

Electrolyte used	Concentration o electrolyte	Distribution Coefficient	Selectivity Coefficient
2:1 Electrolyte			
	0.05 (M)	0.121	7.35×10^{-8}
$MgCl_2$	0.10 (M)	0.107	1.03×10^{-7}
	0.20 (M)	0.097	1.55×10^{-7}
	0.30 (M)	0.087	1.72×10^{-7}
	0.40 (M)	0.077	1.60×10^{-7}
	0.05 (M)	0.125	8.16×10^{-8}
$CaCl_2$	0.10 (M)	0.114	1.25×10^{-7}
	0.20 (M)	0.103	1.89×10^{-7}
	0.30 (M)	0.091	1.97×10^{-7}
	0.40 (M)	0.082	1.93×10^{-7}
	0.05 (M)	0.145	1.18×10^{-7}
$SrCl_2$	0.10 (M)	0.129	3.87×10^{-7}
	0.20 (M)	0.111	2.48×10^{-7}
	0.30 (M)	0.093	2.07×10^{-7}
	0.40 (M)	0.087	2.29×10^{-7}

TABLE -9 (Contd..)

Electrolyte used	Concentration of electrolyte	Distribution Coefficient	Selectivity Coefficient
	0.05 (M)	0.171	2.11×10^{-7}
$BaCl_2$	0.10 (M)	0.148	2.78×10^{-7}
	0.20 (M)	0.121	3.07×10^{-7}
	0.30 (M)	0.104	2.94×10^{-7}
	0.40 (M)	0.093	2.81×10^{-7}
Quaternary Ammonium Salt			
	0.05 (M)	2.52×10^{-2}	2.65×10^{-8}
TMABr	0.10 (M)	1.73×10^{-2}	2.53×10^{-8}
	0.20 (M)	1.18×10^{-2}	2.38×10^{-8}
	0.30 (M)	9.47×10^{-3}	2.30×10^{-8}
	0.40 (M)	7.89×10^{-3}	2.15×10^{-8}
	0.05 (M)	4.73×10^{-2}	9.52×10^{-8}
TEABr	0.10 (M)	2.92×10^{-2}	7.33×10^{-8}
	0.20 (M)	1.77×10^{-2}	5.48×10^{-8}
	0.30 (M)	1.31×10^{-2}	4.55×10^{-8}
	0.40 (M)	1.08×10^{-2}	4.16×10^{-8}

TABLE - 9 (Contd..)

Electrolyte used	Concentration of electrolyte	Distribution Coefficient	Selectivity Coefficient
	0.05 (M)	6.15×10^{-2}	1.63×10^{-7}
TPABr	0.10 (M)	3.79×10^{-2}	1.25×10^{-7}
	0.20 (M)	2.40×10^{-2}	1.03×10^{-7}
	0.30 (M)	1.81×10^{-2}	8.94×10^{-8}
	0.40 (M)	1.54×10^{-2}	8.78×10^{-8}
	0.05 (M)	8.83×10^{-2}	3.46×10^{-7}
TBABr	0.10 (M)	5.21×10^{-2}	2.44×10^{-7}
	0.20 (M)	3.15×10^{-2}	1.83×10^{-7}
	0.30 (M)	2.36×10^{-2}	1.56×10^{-7}
	0.40 (M)	1.89×10^{-2}	1.36×10^{-7}
	2×10^{-4}	3.964	2.57×10^{-6}
DDTMABr	4×10^{-4}	3.025	3.04×10^{-6}
	6×10^{-4}	2.367	2.80×10^{-6}
	8×10^{-4}	1.974	2.60×10^{-6}
	1×10^{-3}	1.737	2.53×10^{-6}

TABLE - 9 (Contd..)

Electrolyte used	Concentration of electrolyte	Distribution Coefficient	Selectivity Coefficient
	2×10^{-4} (M)	18.419	5.91×10^{-5}
CTMABr	4×10^{-4} (M)	12.391	5.48×10^{-5}
	6×10^{-4} (M)	9.571	4.99×10^{-5}
	8×10^{-4} (M)	7.702	4.35×10^{-5}
	1×10^{-3} (M)	6.423	3.81×10^{-5}
	1×10^{-4} (M)	7.929	1.04×10^{-5}
DDPBr	2×10^{-4} (M)	5.405	9.86×10^{-6}
	3×10^{-4} (M)	4.039	8.31×10^{-6}
	4×10^{-4} (M)	3.291	7.39×10^{-6}
	5×10^{-4} (M)	2.843	6.93×10^{-6}
	1×10^{-4} (M)	27.225	1.33×10^{-4}
CPBr	2×10^{-4} (M)	16.478	1.11×10^{-4}
	3×10^{-4} (M)	11.854	8.07×10^{-5}
	4×10^{-4} (M)	9.348	6.60×10^{-5}
	5×10^{-4} (M)	7.634	5.52×10^{-5}

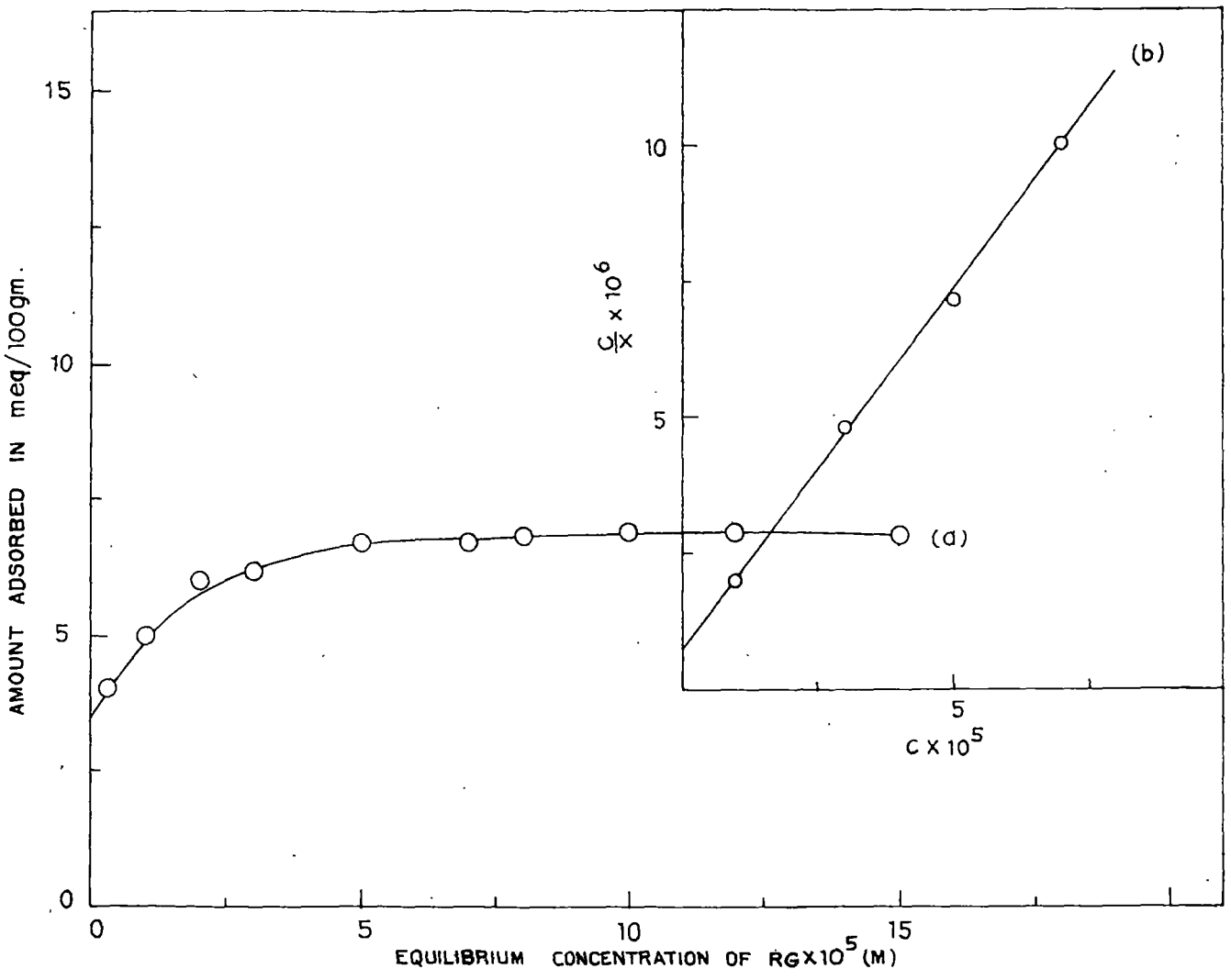

FIG. 25. ADSORPTION ISOTHERM AT 28°C (a) LANGMUIR PLOT (b) OF RG ON Na-KAOLINITE .

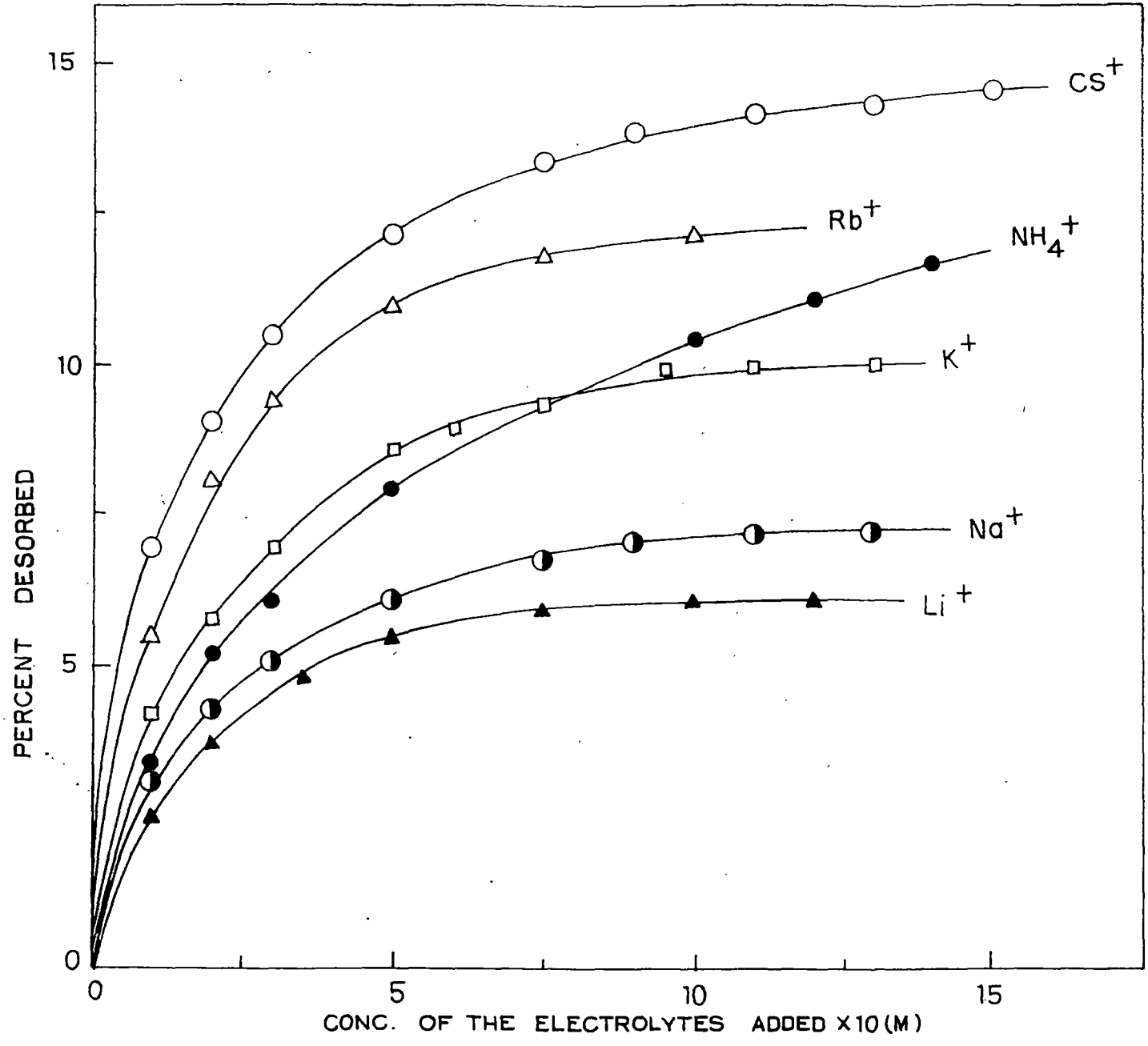

FIG. 26. DESORPTION OF RG FROM Na-KAOLINITE-RG BY VARIOUS MONOVALENT IONS.

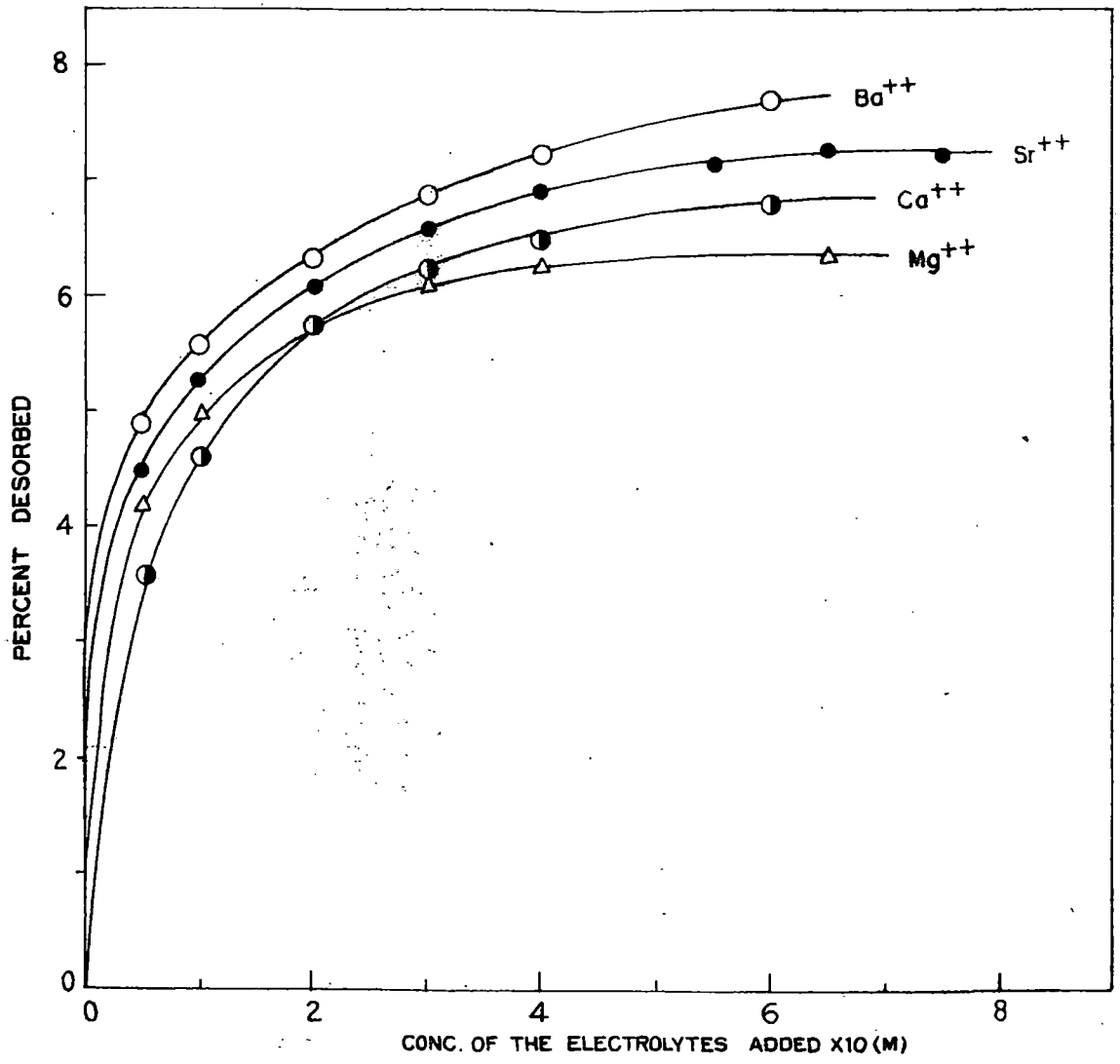

FIG. 27. DESORPTION OF RG FROM Na- KAOLINITE-RG BY VARIOUS BIVALENT IONS.

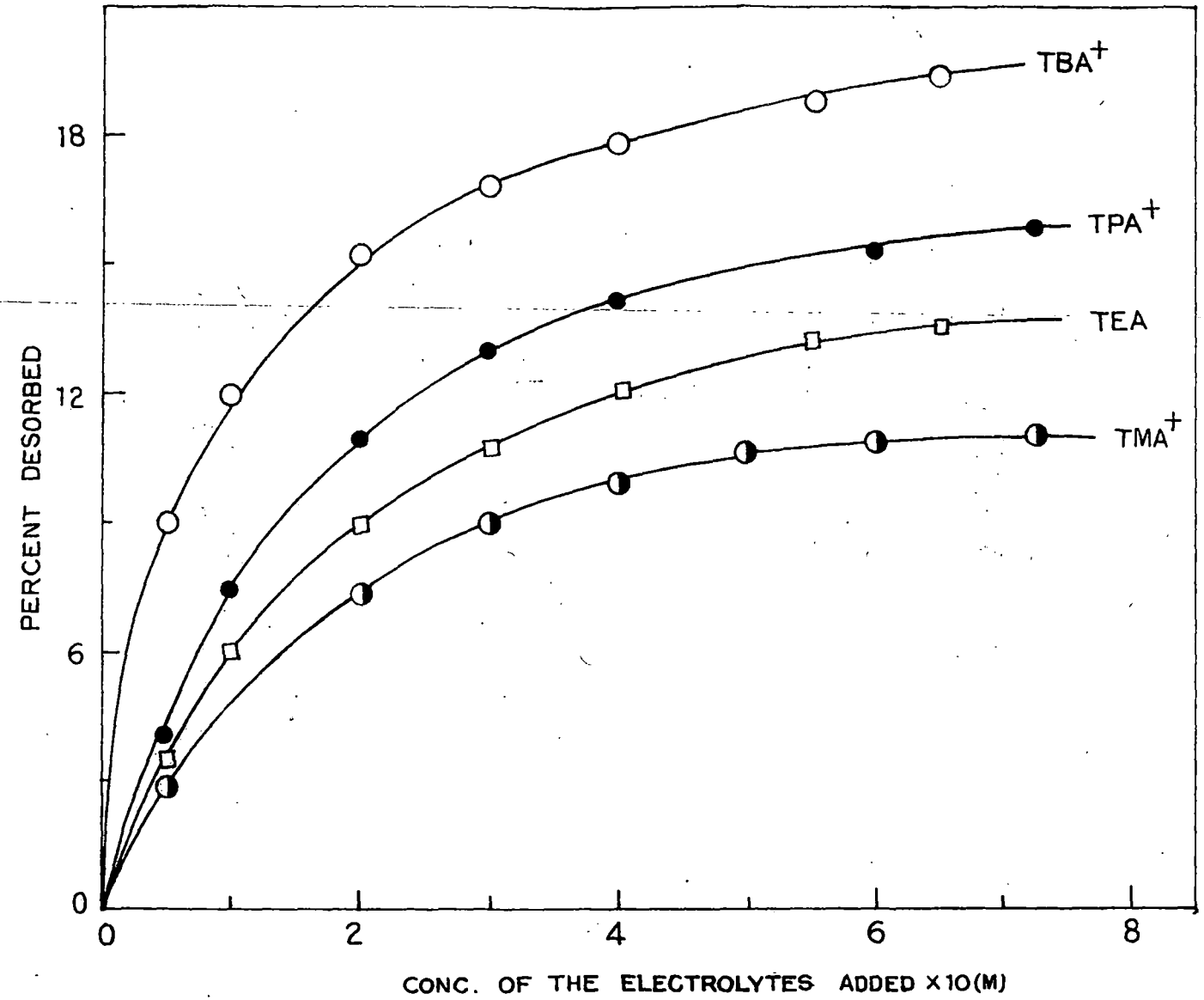

FIG. 28. DESORPTION OF RG FROM Na-KAOLINITE-RG BY VARIOUS TETRA-ALKYL AMMONIUM HALIDES.

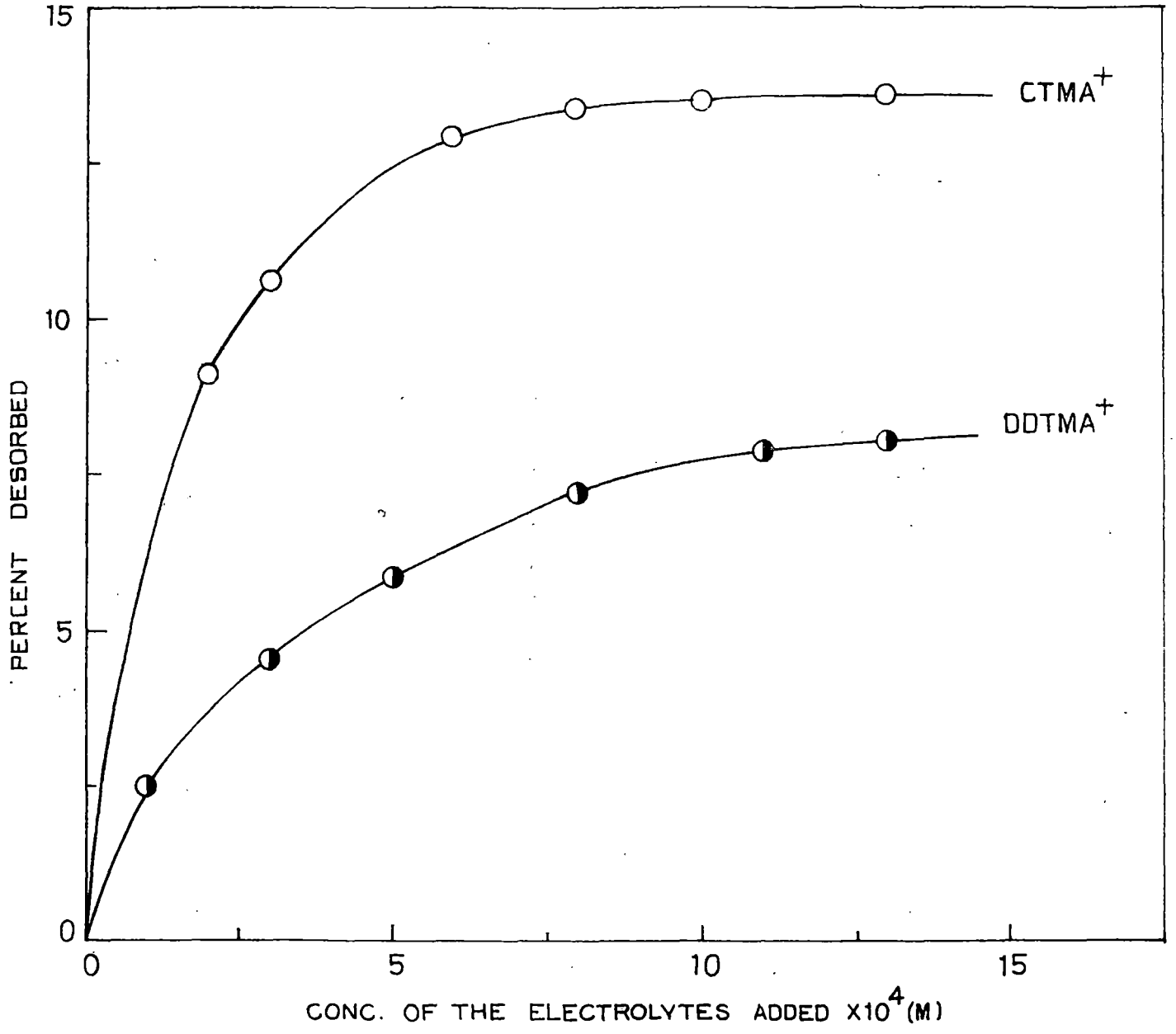

FIG. 29. DESORPTION OF RG FROM Na-KAOLINITE - RG BY VARIOUS LONG-CHAIN SURFACE ACTIVE ALKYLTRIMETHYLAMMONIUM HALIDES.

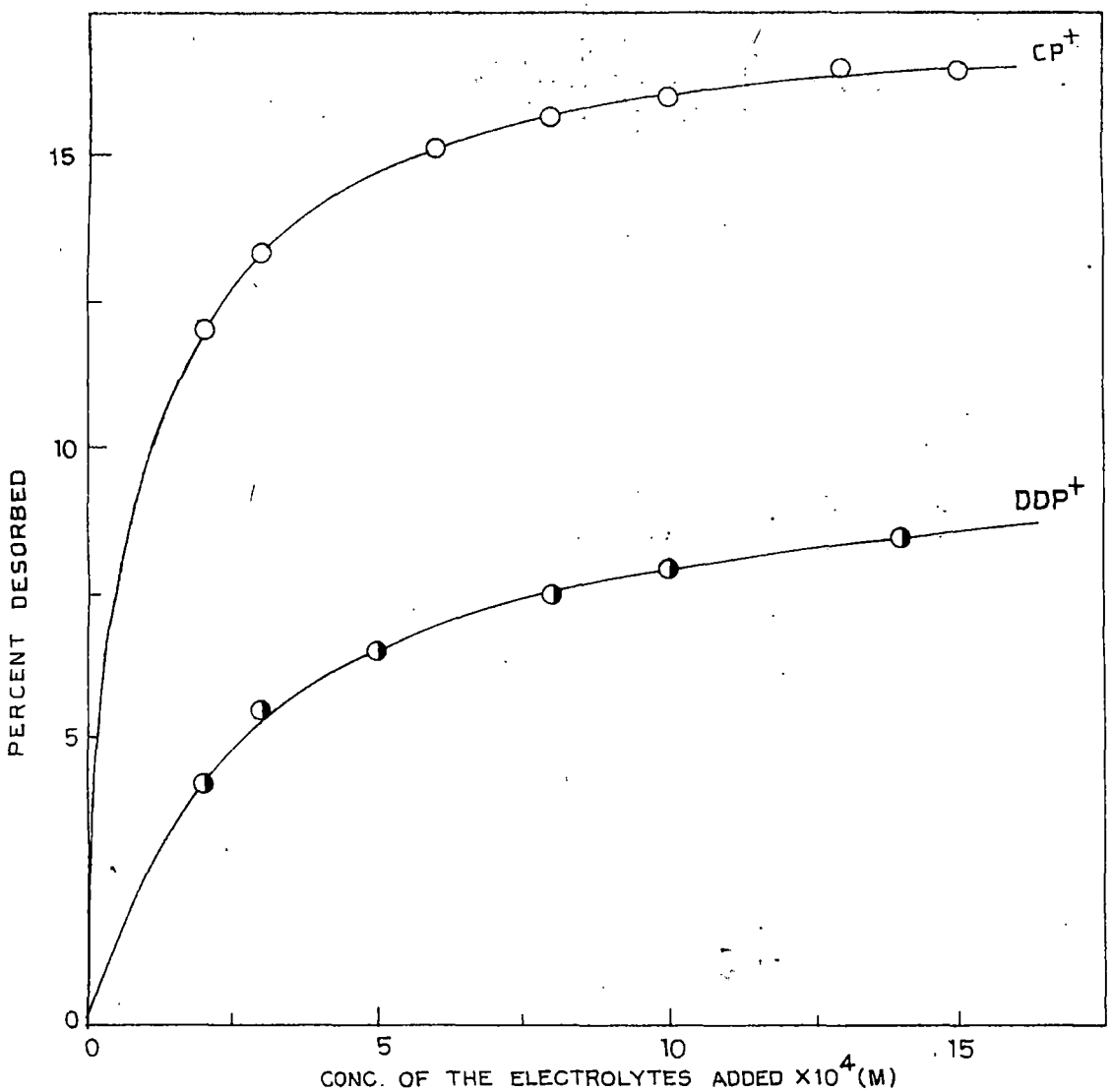

FIG. 30. DESORPTION OF RG FROM Na-KAOLINITE-RG BY VARIOUS LONG-CHAIN SURFACE ACTIVE ALKYLPYRIDINIUM HALIDES.

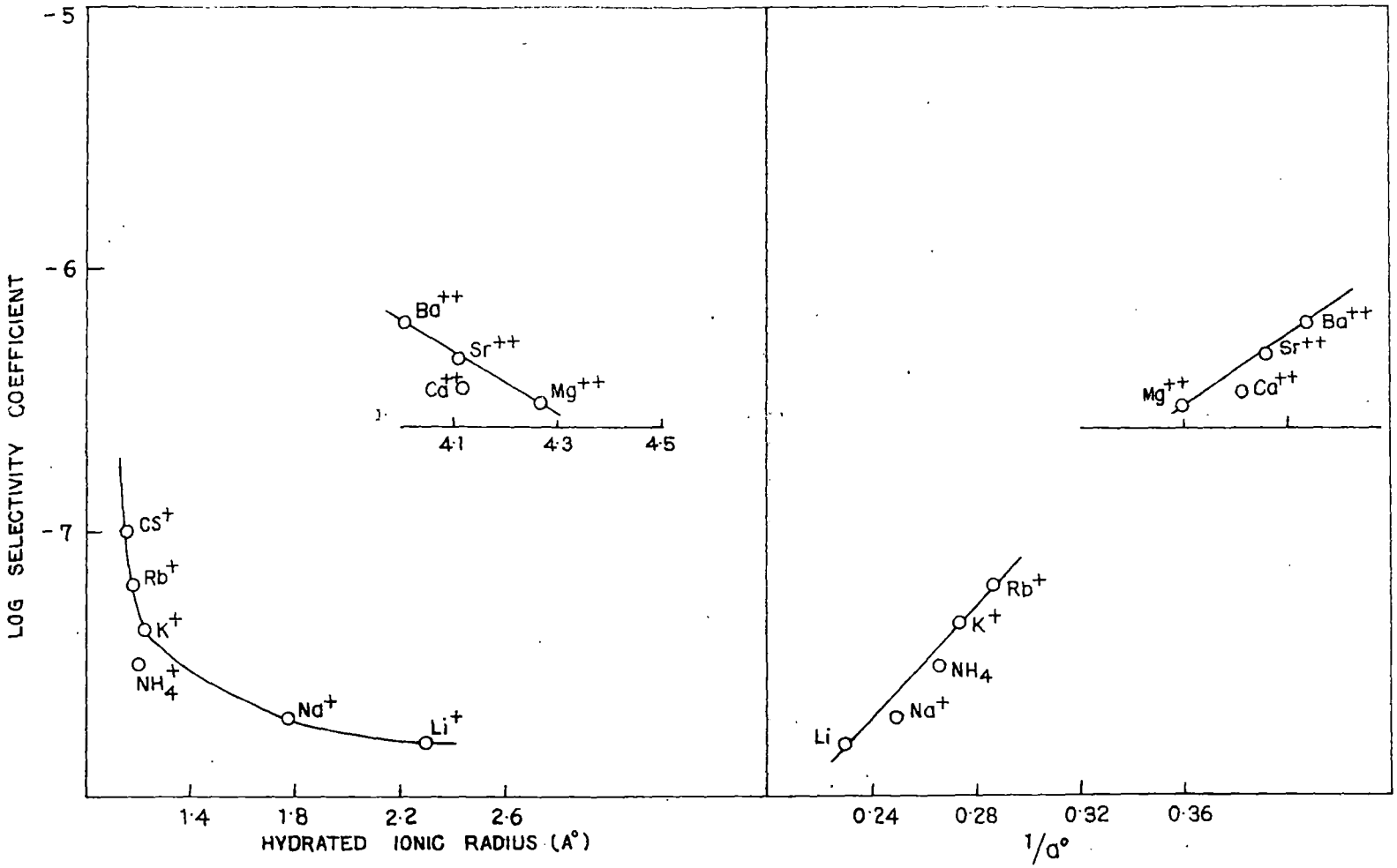

FIG. 31. CORRELATION OF SELECTIVITY COEFFICIENT WITH HYDRATED IONIC RADIUS AND DEBYE-HUCKEL PARAMETER, a°, IN THE DESORPTION OF RG FROM Na-KAOLINITE-RG.

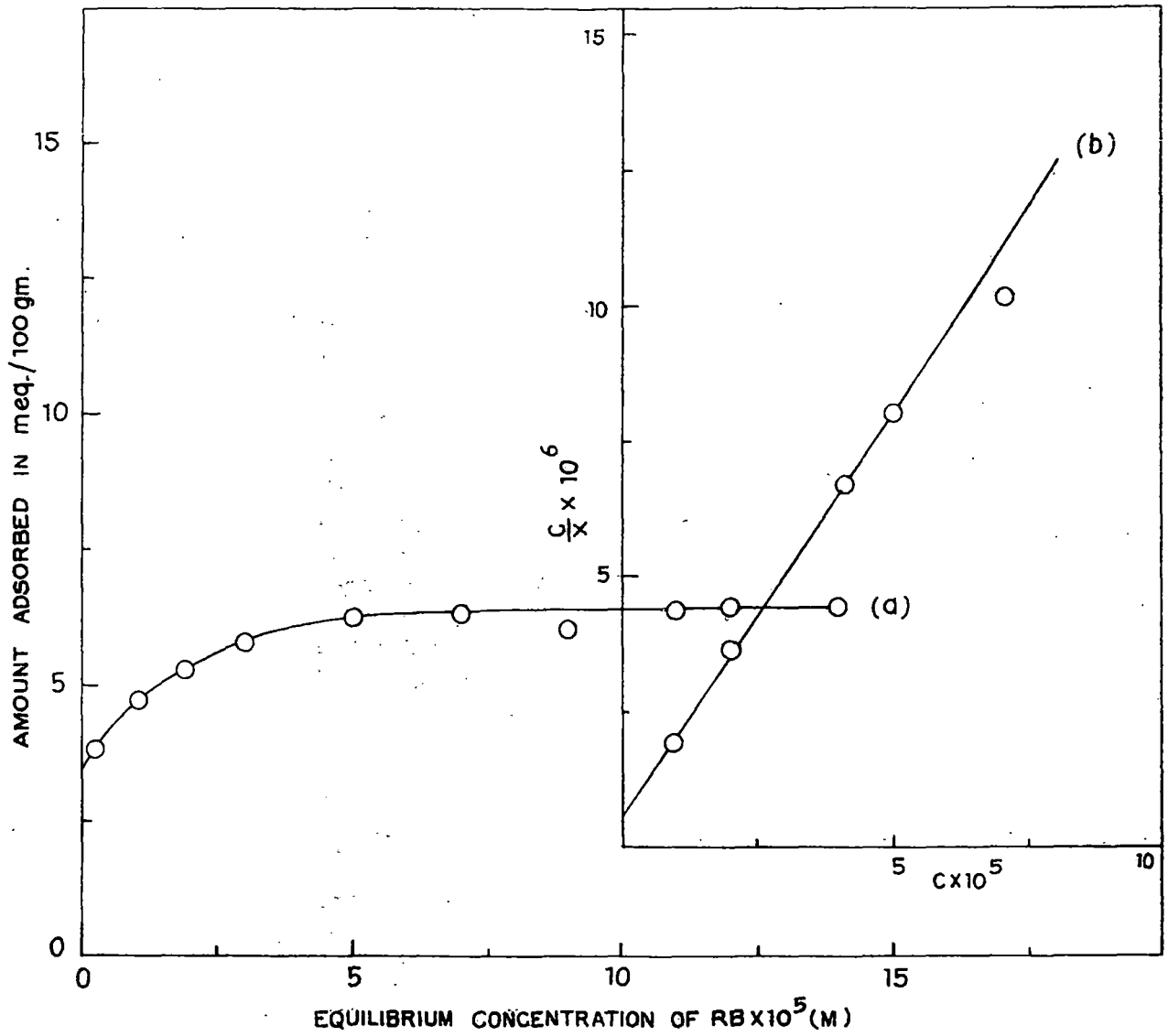

FIG. 32. ADSORPTION ISOTHERM AT 28°C (a) AND LANGMUIR PLOT (b) OF RB ON Na-KAOLINITE.

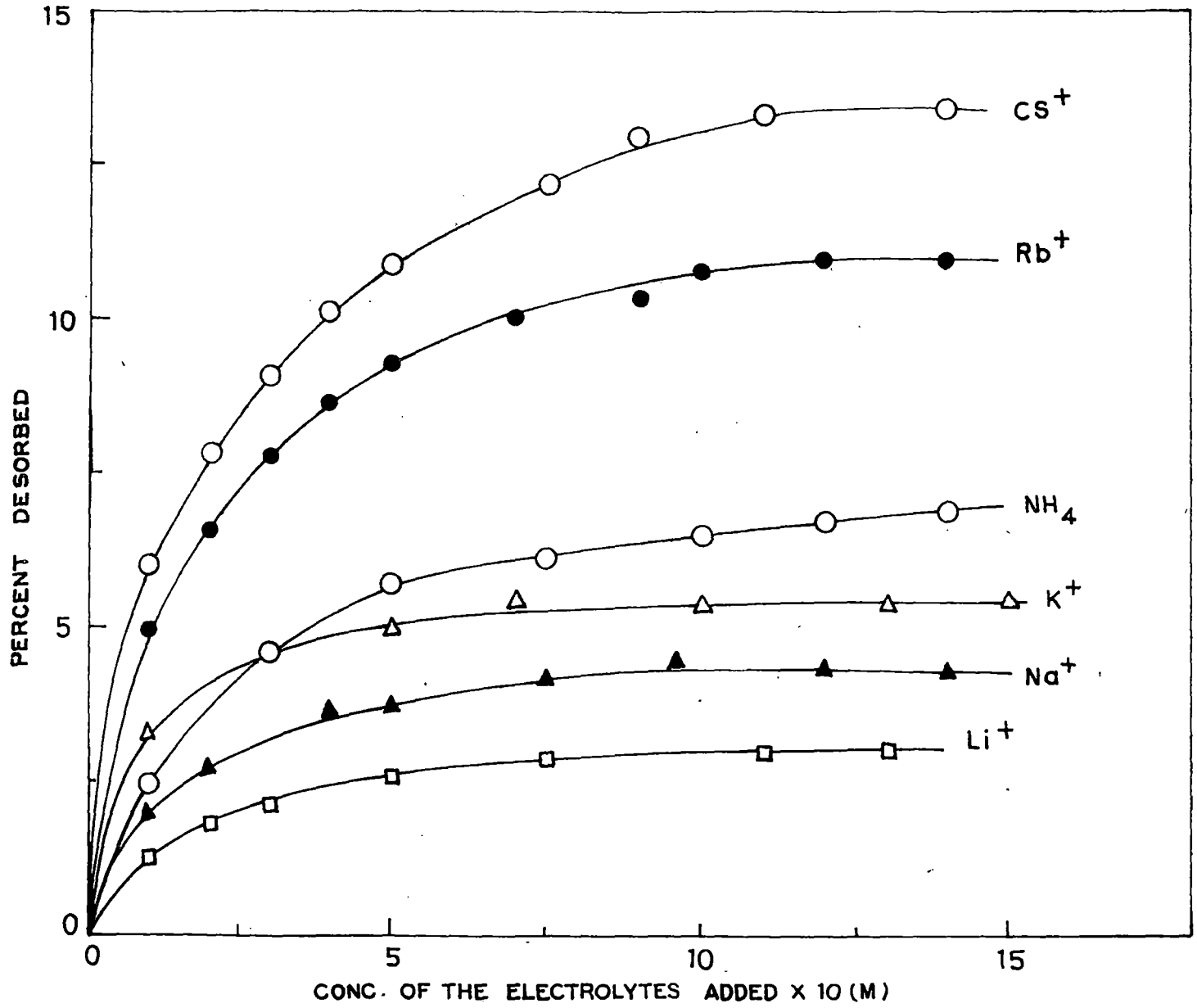

FIG. 33. DESORPTION OF RB FROM Na-KAOLINITE-RB BY VARIOUS MONOVALENT IONS.

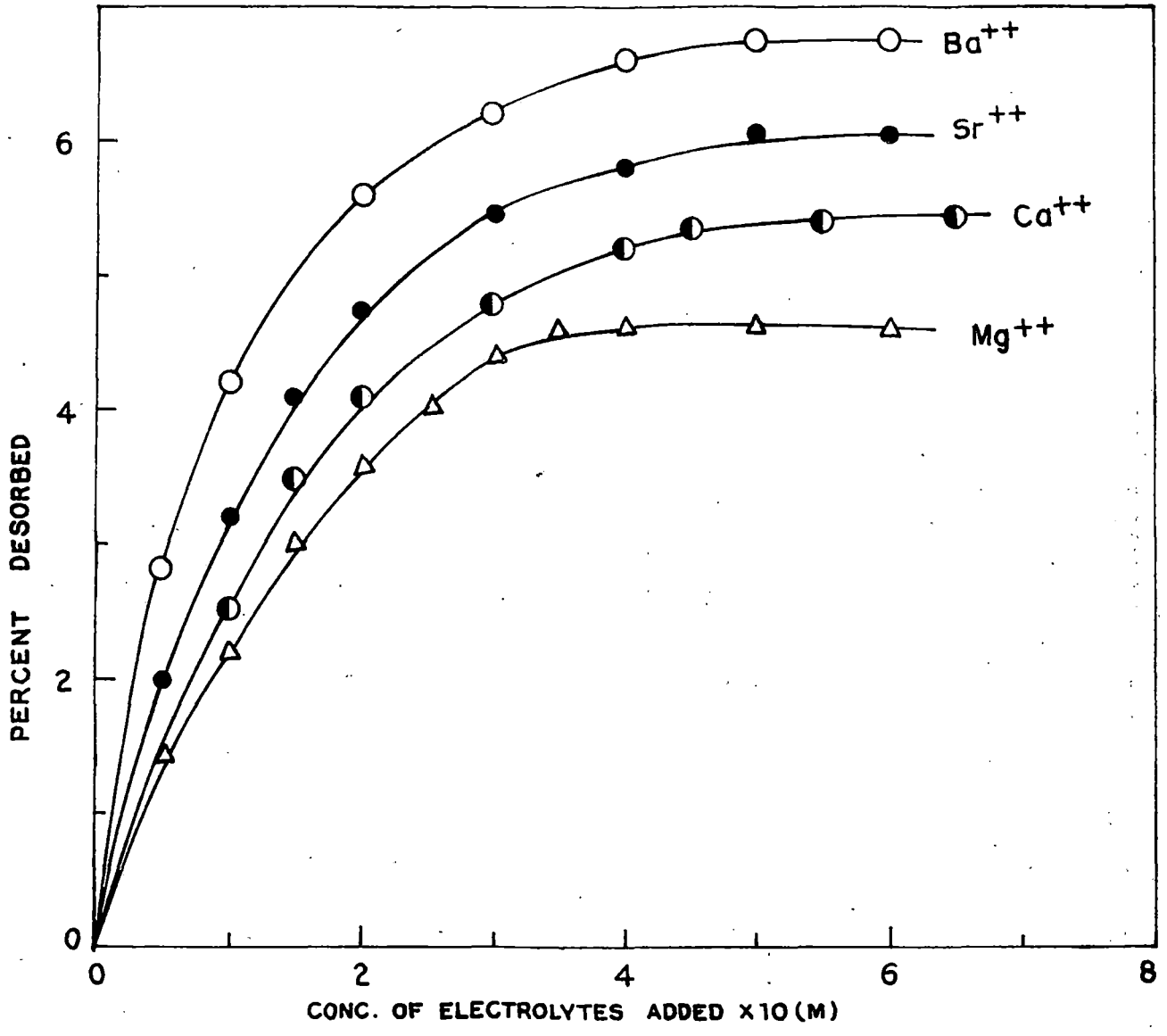

FIG. 34. DESORPTION OF RB FROM Na- KAOLINITE - RB BY VARIOUS BIVALENT IONS.

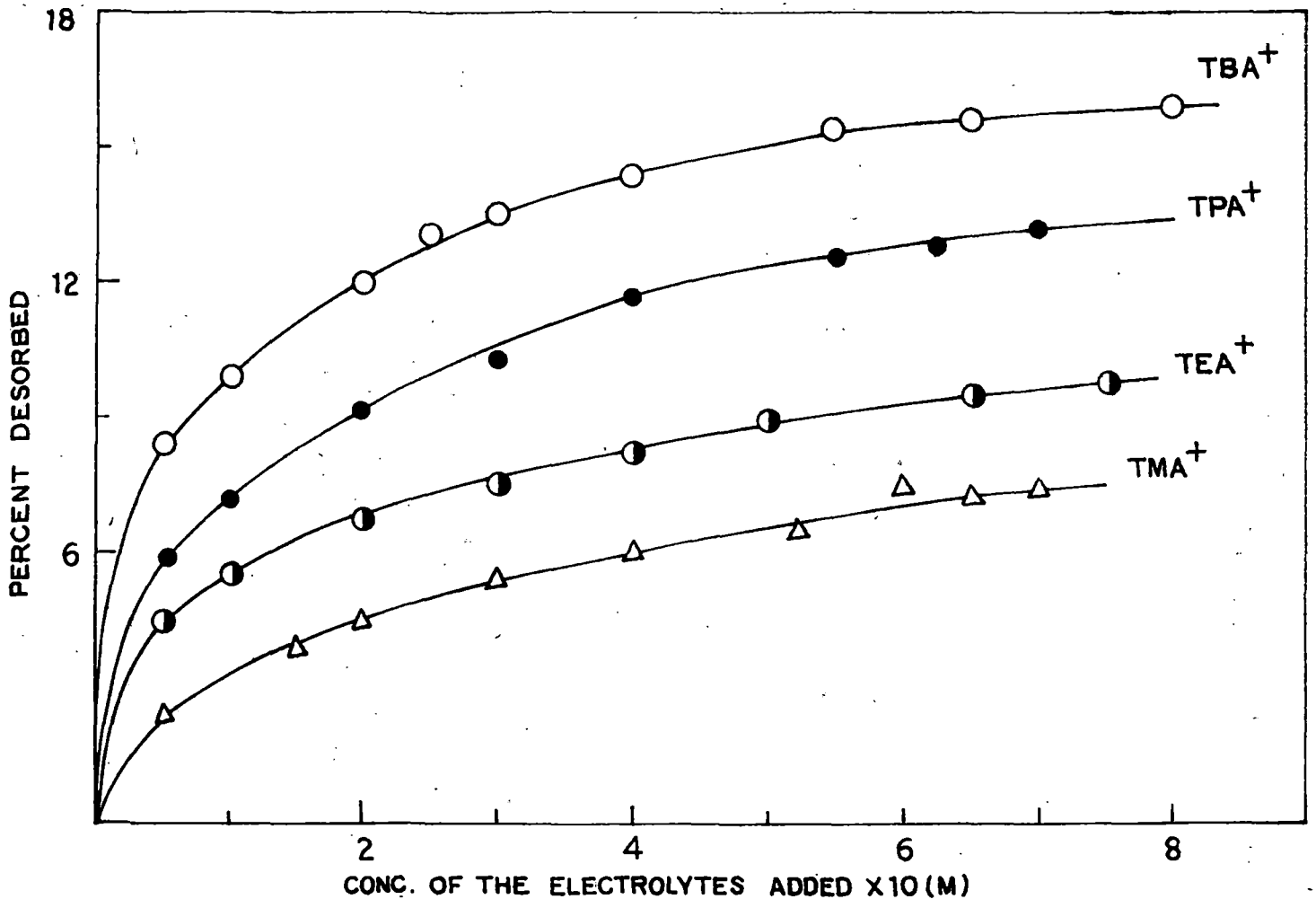

FIG. 35. DESORPTION OF RB FROM Na-KAOLINITE RB BY VARIOUS TETRA ALKYL-AMMONIUM HALIDES.

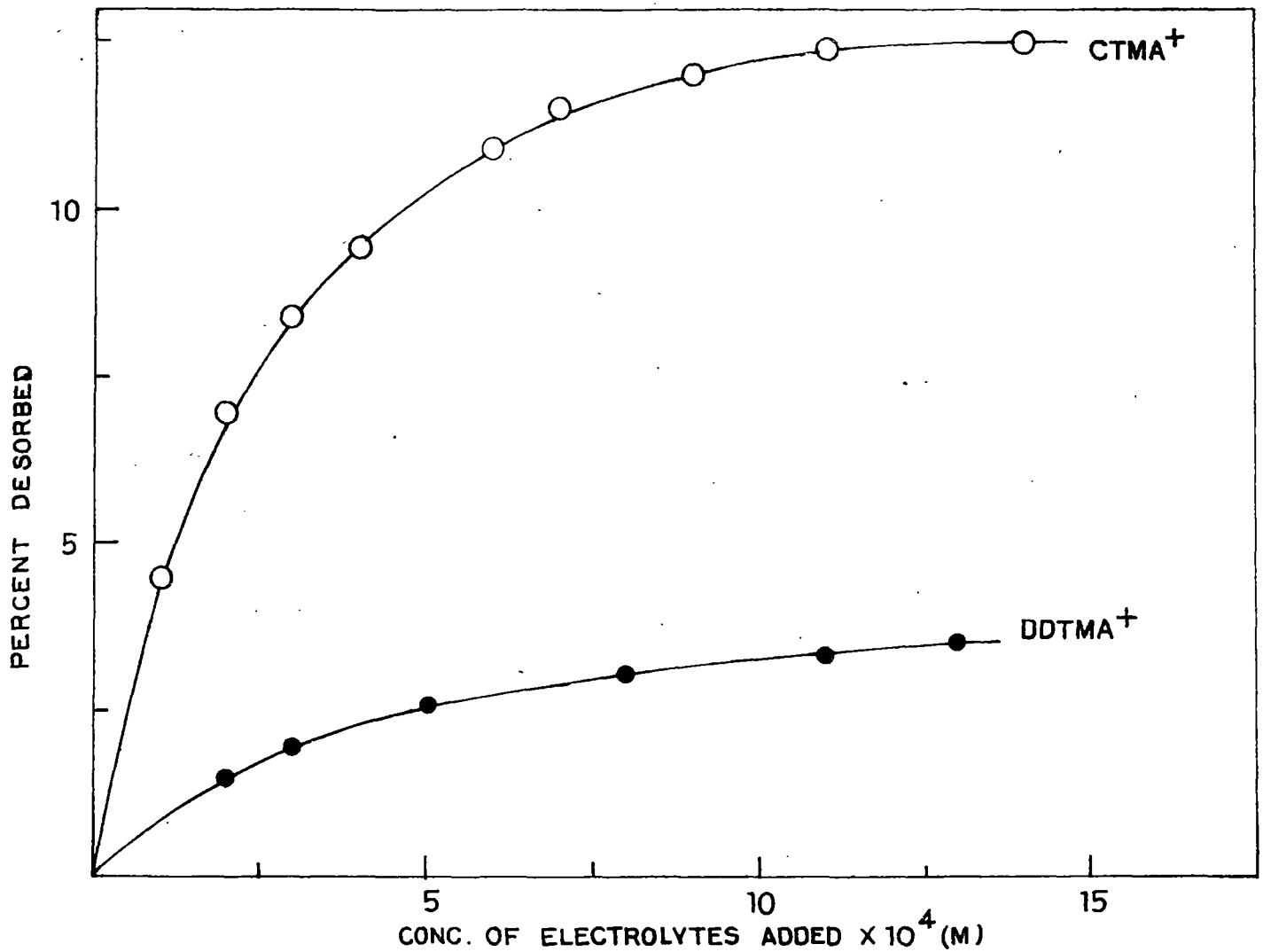

FIG. 36. DESORPTION OF RB FROM Na-KAOLINITE BY VARIOUS LONG-CHAIN SURFACE ACTIVE ALKYLTRIMETHYL AMMONIUM HALIDES.

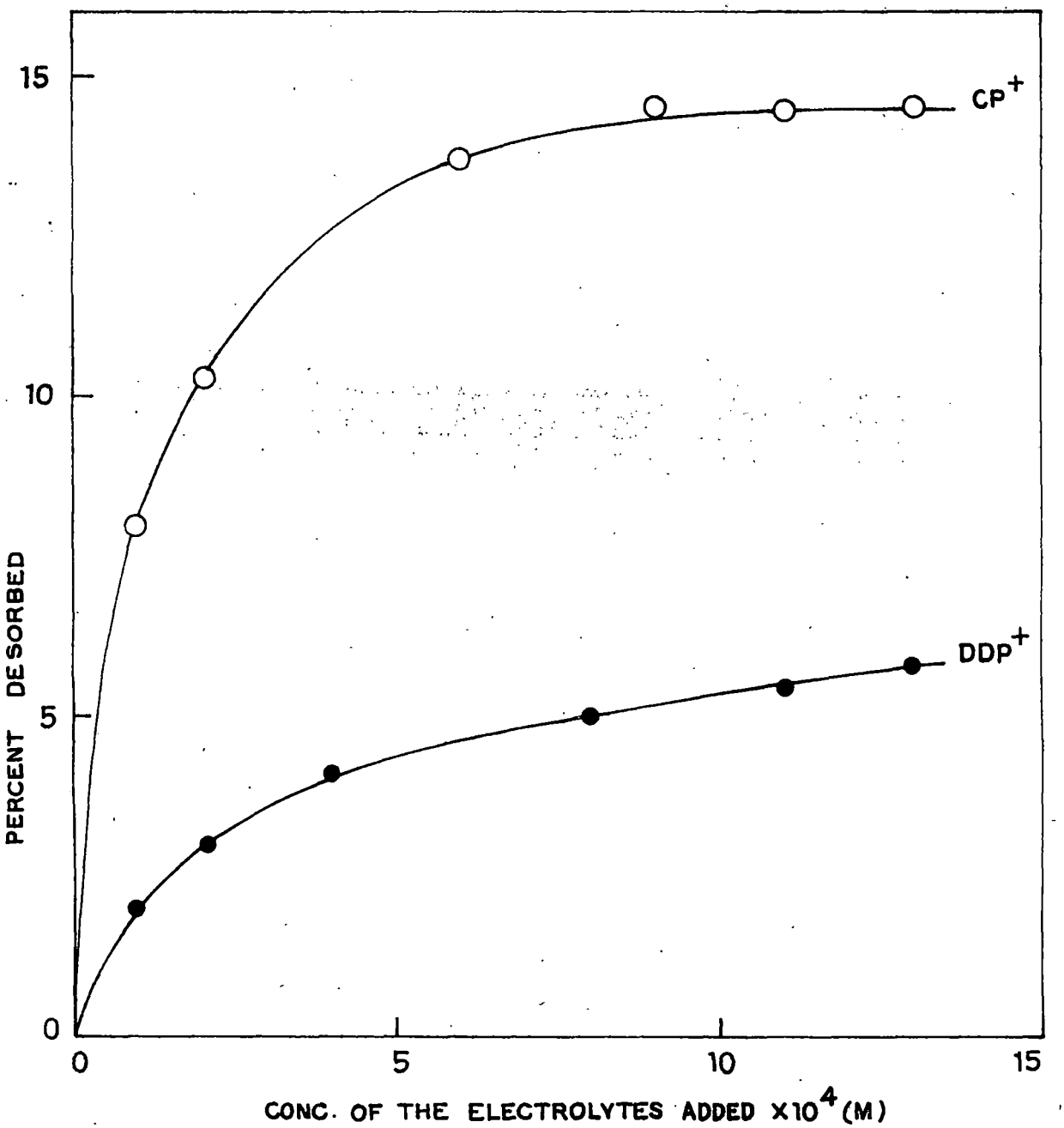

FIG. 37. DESORPTION OF RB FROM Na-KAOLINITE-RB BY VARIOUS LONG-CHAIN SURFACE ACTIVE ALKYLPYRIDINIUM HALIDES.

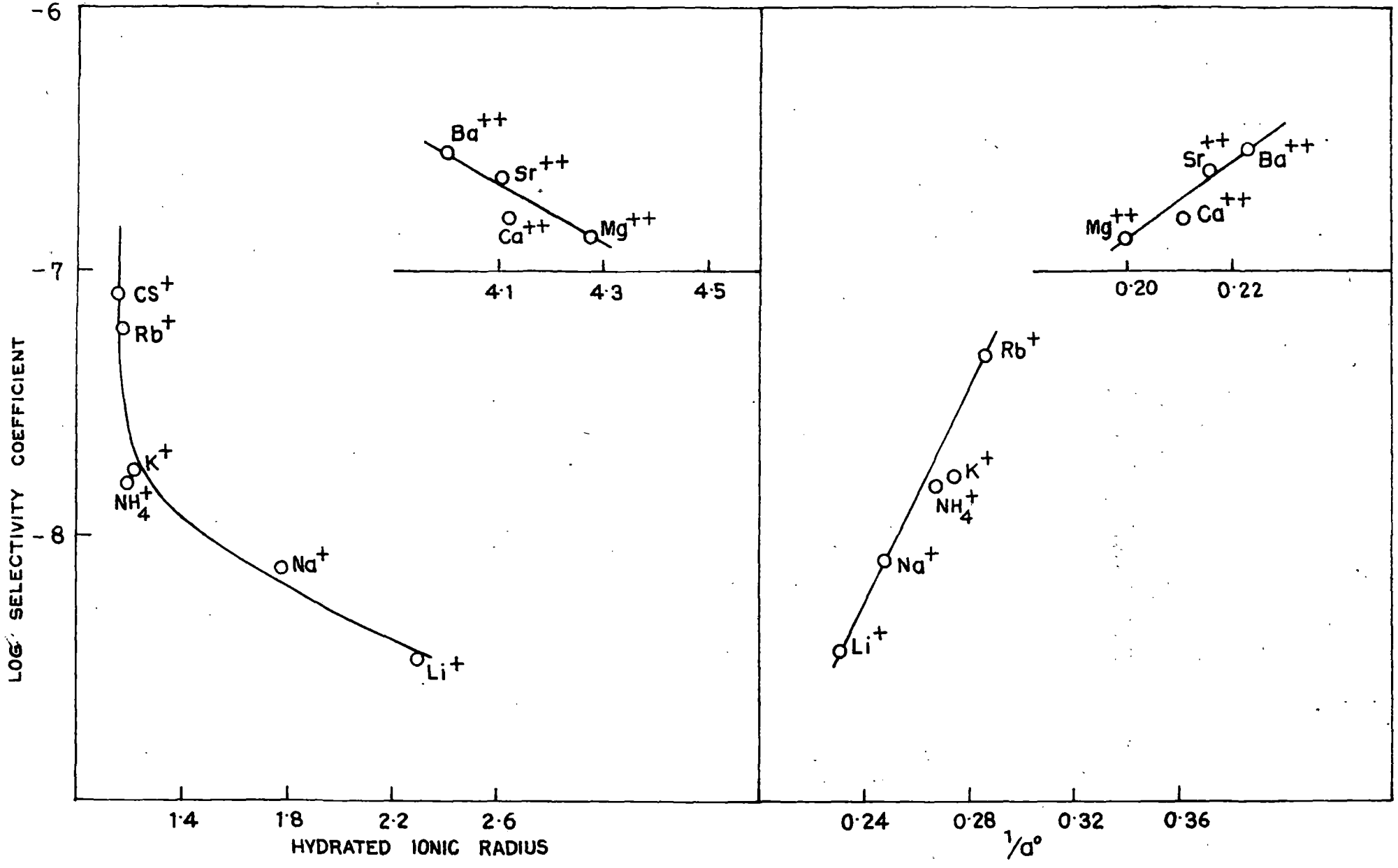

FIG. 38. CORRELATION OF SELECTIVITY COEFFICIENT WITH HYDRATED IONIC RADIUS AND DEBYE-HUCKEL PARAMETER, a°, IN THE DESORPTION OF RB FROM Na- KAOLINITE - RB.

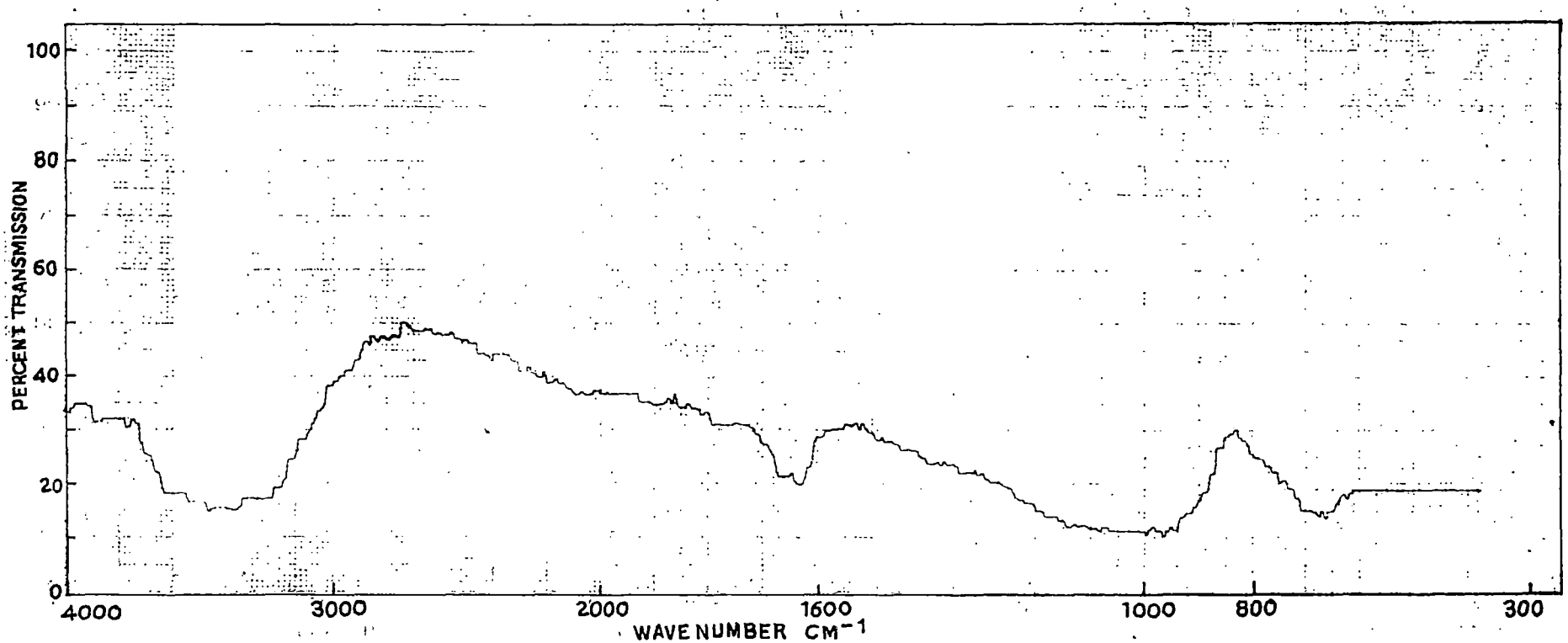

Fig. 39. Infrared Spectrum of Na-Kaolonite

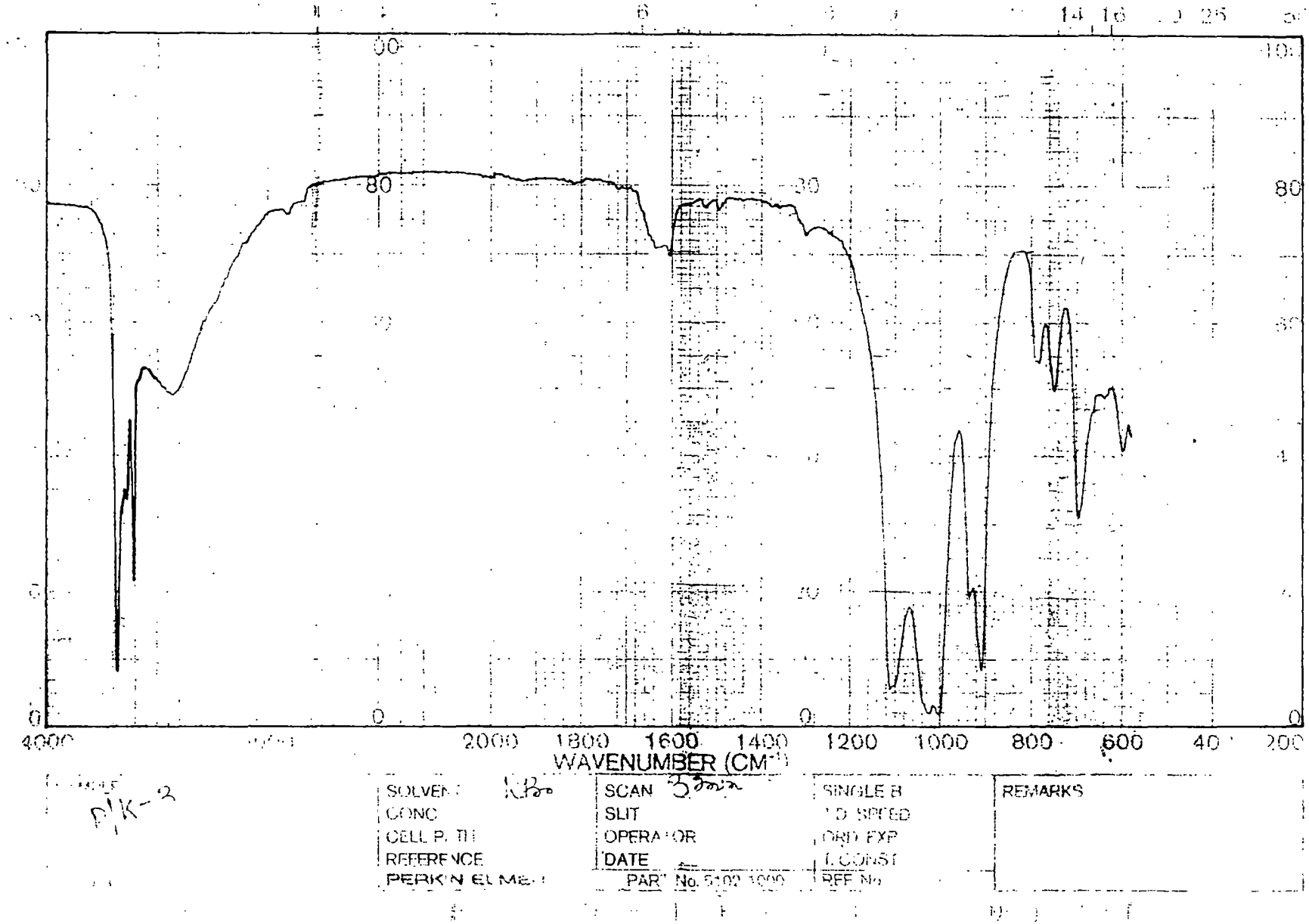

Fig. 40. Infrared spectrum of 100% exchanged Na-Kaolinite-RG (in KBr pellet).

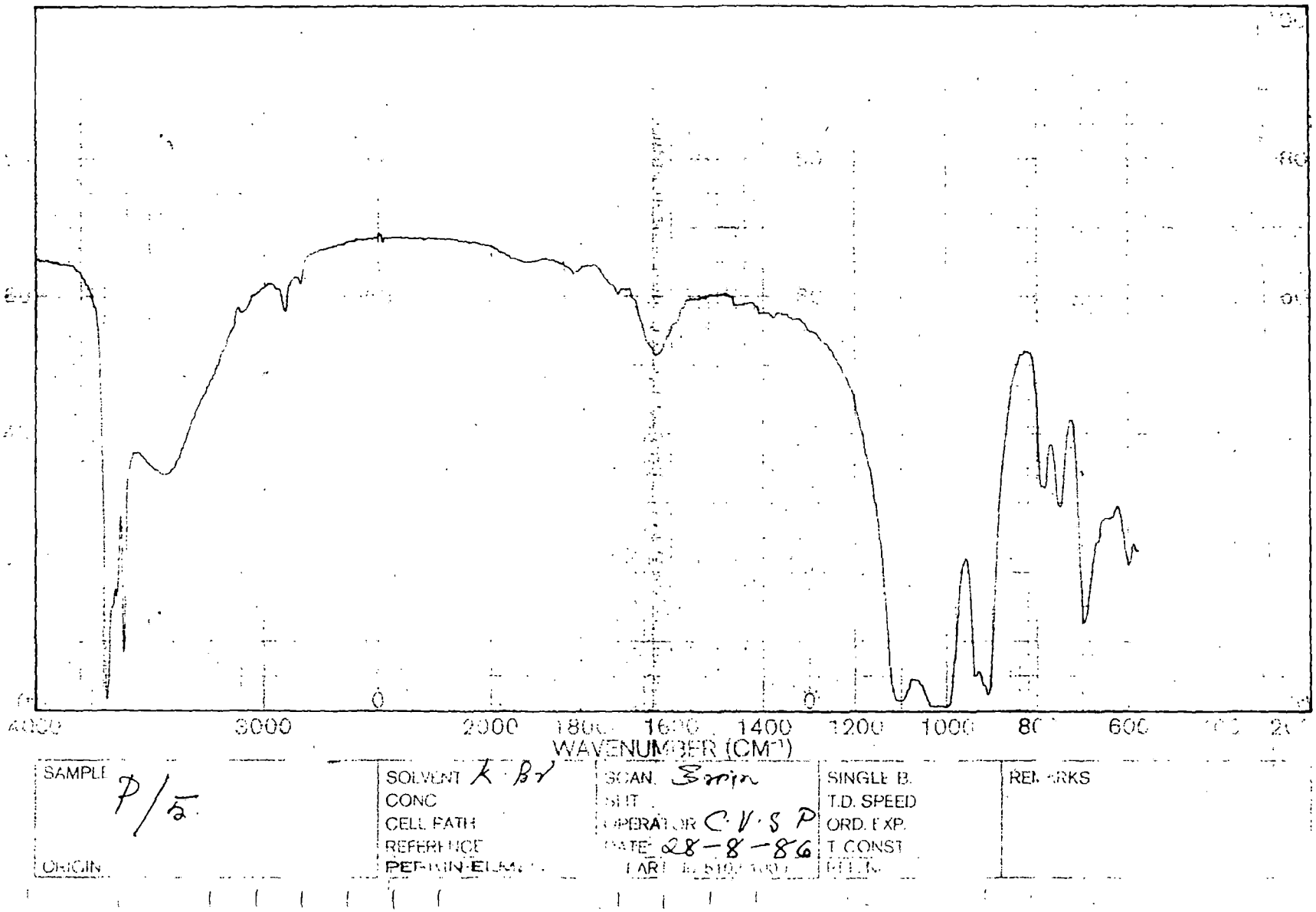

Fig. 41. Infrared spectrum of 100% exchanged Na- Kaolinite - RB (in KBr pellet) .